A novel method for measurement of the angle of repose of granular seeds in discrete element methods

Xin Du,[1,2] Cailing Liu,[2] Changqing Liu,[1] Qixin Sun,[1] Shufa Chen[1]

[1]School of Mechanical Engineering, Jiangsu Ocean University, Lianyungang; [2]College of Engineering, China Agricultural University, Beijing, China

Abstract

Discrete element numerical simulations can help researchers find potential problems in the design phase, shortening the development cycle and reducing costs. In the field of agricultural engineering, more and more researchers are using discrete element methods (DEM) to assist in designing and optimising equipment parameters. Model parameters calibration is a prerequisite for discrete element numerical calculations, and the angle of repose (AoR) is commonly used to calibrate the parameters. However, the measurement of AoR in DEM was not seriously considered in industrial or academic fields. In practice, AoR is measured manually, using 2D digital image processing or using a 3D scan. However, reliable and consistent measurements of AoR in DEM are rarely mentioned. This study suggests an accurate and consistent way to measure AoR in DEM using a novel method to read particle coordinate information directly from the data file; then, the AoR is calculated by linearly fitting the centre coordinates of the outermost particles. Influences of input variables on AoR acquisition are discussed through several examples using customised templates with known angles. Then a comparative study of the accuracy of the measurement of AoR in DEM and the reliability of the parameter calibration results by the manual measurement, 2D digital image processing, and algorithm proposed in this paper was conducted. In case studies with four seed materials, this method prevented the subjective selection of AoR, improved the identification accuracy, and increased the precision and accuracy of DEM calibration. In addition, the time consumption for obtaining AoR using the novel method for measurement is much less than that of 2D.

Correspondence: Cailing Liu, College of Engineering, China Agricultural University, Beijing 100083, China.
E-mail: cailingliu@163.com

Key words: angle of repose, discrete element methods, automated measurement, seeds, novel algorithm.

Conflict of interest: the authors declare no potential conflict of interest.

Acknowledgements: this work was financially supported by the National Key Research and Development Plan of China (2017YFD0700703-03).

Received: 31 August 2022.
Accepted: 23 November 2022.

Journal of Agricultural Engineering 2023; LIV:1504
doi:10.4081/jae.2023.1504

Introduction

In the field of agricultural engineering, more and more researchers are using discrete element methods (DEM) to assist in designing and optimising equipment parameters (Sun *et al*., 2022). To study the shooting performance of the kinds of wheat, Wang *et al*. (2022) conducted DEM-CFD coupling simulation experiments. Gao *et al*. (2021) studied the motions of maize particles in a novel high-speed seed metering device based on the DEM. Based on coupled simulations using CFD and DEM, Hu *et al*. (2021) conducted a numerical study of various structural and working parameters of an air-assisted centralised seed-metering device. Wang *et al*. (2020) used the DEM to simulate vibrating tillage to gain a clear understanding of the dynamic forces and soil behaviour of vibratory tools.

Model parameters calibration is a prerequisite for discrete element numerical calculations, and the angle of repose (AoR) is commonly used to calibrate the parameters. However, the measurement of AoR in DEM was not seriously considered in industrial or academic fields (Roessler and Katterfeld, 2018). For example, as shown in Figure 1A, the stacking of particles can be produced in many ways, such as 'emptying,' 'submerging,' 'piling,' and 'pouring' (Frączek *et al.*, 2007). Regardless of the different formation processes of the static particle heap, the value of AoR can be obtained by reading the heap's surface value directly by a protractor or calculating the deal with the measured heap's diameter and height (Geldart *et al.,* 2006; Frączek *et al*., 2007; Qi, Chen, and Sadek, 2019). In most recent cases, the quoted authors invoke optical methods inherent in image analysis carried out based on a single or a set of pictures. For example, the boundary contours of the particle pile images were extracted by performing greyscale and binarization, then using the least-squares method, the fitted equations were obtained by linear fitting, and the AoR was calculated by the arctangent function (Frączek *et al*., 2007; Cheng and Zhao, 2017; Li *et al.*, 2017; Wójcik *et al*., 2018; Li *et al.*, 2020; Cao *et al.*, 2021). Now several research groups proposed 3D coordinate measurement, and the measured object of which a set of digital photographs has been made can be viewed as a 3D model and subsequently subjected to analysis characteristics of coordinate metrology (Figure 1B) (Rackl *et al*., 2017; Wójcik *et*

al., 2018, 2019; Tan *et al*., 2020; Klanfar *et al*., 2021). Among the methods described above, only the first two can be used to measure the AoR in the DEM software, and the last way is only applicable to measure the AoR of the actual object. However, two unneglectable problems are lower repeatability (errors between two measurements performed by one operator) and lower reproducibility (errors between the measurements by different operators in different laboratories). Considering the significant influences of interaction properties, particle-wall interaction, or intergranular interaction on the AoR, the calibration based on unreliable measurements of DEM values could lead to quite distorted simulation results (Tan *et al*., 2021). Due to the weakness and nonstandard calibration of parameters based on the comparison between measured and simulated AoR, more precise and reliable calibration is necessary to simulate irregular materials in DEM industrial applications (Marigo and Stitt, 2015). Considering the above analysis, the authors decided to propose a novel method for precise measurement of the AoR of granular seed materials in DEM. Our study aims to provide an efficient and standard calibration method with reduced time cost and increased repeatability.

Materials and Methods

As shown in Figure 2, in this paper: i) four seeds were selected as the objects of study; ii) briefly introduced the basic model of DEM; iii) the DEM models for seed and stacking angle tests were established; iv) elaborated the Python-based AoR measurement method; v) using a fixed-angle template to find the optimisation of the measured parameters; vi) comparing the AoR values obtained by the three methods of the algorithm presented in this paper (DEMpy), digital image analysis (2D), and manual measurements using a virtual protractor (MVM).

Material characteristics of seeds

The investigated seeds (including maize, rice, soybean, and wheat) were selected from seed varieties widely grown in China, contributing to the differences in AoR. Figure 3 shows photographs of four representative seed materials with different basic particle shapes and size distributions. All relevant properties are listed in Table 1, where Poisson's ratio and shear modulus of each material is taken from references, bulk density, particle density,

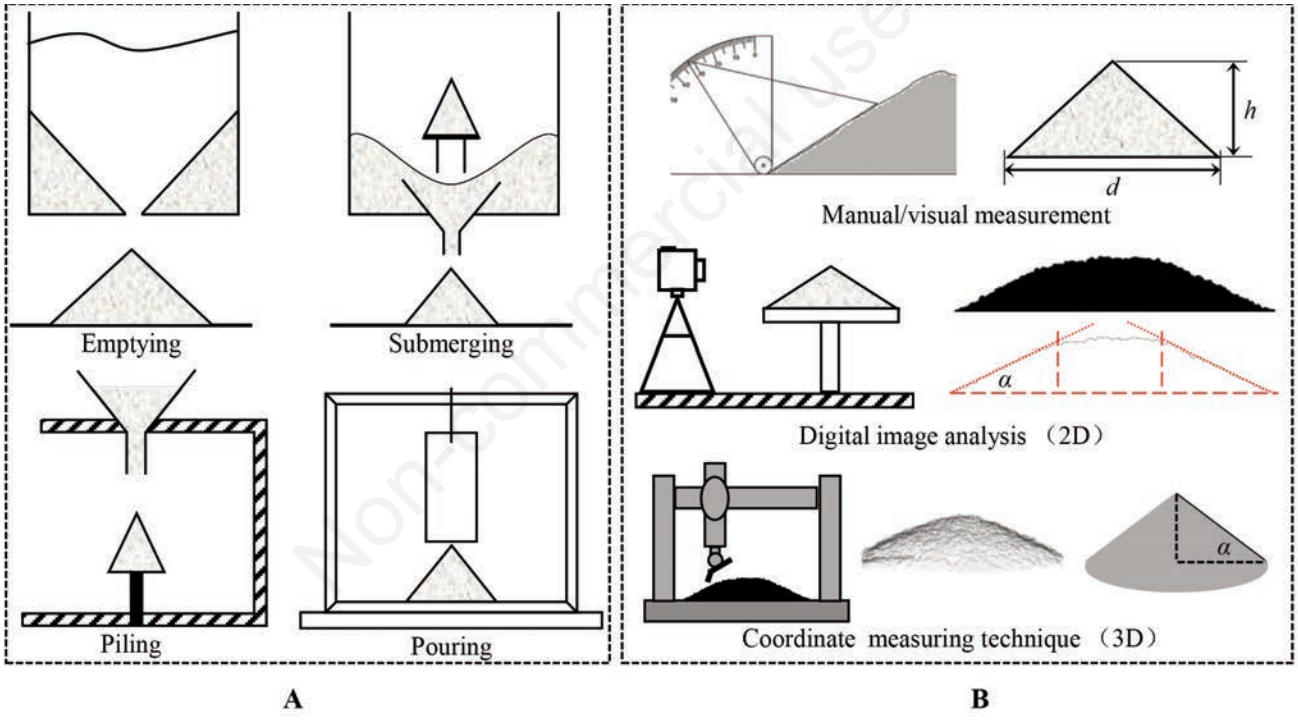

Figure 1. Methods of cone formation (**A**), the angle of repose acquisition method (**B**).

Table 1. Discrete element parameters.

Parameters	Soybean (Jia *et al*., 2018)	Rice (Lu *et al*., 2016)	Wheat (Liu *et al*., 2019)	Maize (Ding *et al*., 2019)	Wall (Liu *et al*., 2018; Zhu *et al*., 2018)
Poisson's ratio	0.40	0.3	0.42	0.40	0.394
Shear modulus, Pa	6.1×10^8	1.8×10^8	5.1×10^7	1.3×10^8	8.9×10^8
Bulk density, kg/cm^3	761.3	619.5	752.1	750.2	1060
Particle density, kg/cm^3	1202.1	1109.6	1236.2	1184.2	-
Moisture, %	11.4	12.3	11.6	12.5	-

and moisture content are measured experimentally; the measurement method is consistent with the literature (Mousaviraad and Tekeste, 2020; Kalman and Portnikov, 2021) and will not be repeated in this paper.

One hundred seeds were randomly selected among the above seeds, and their length, width, and thickness were measured using a digital display vernier calliper. The shape distribution of maize seeds varies into flat and round with length × width × thickness of 11.38×8.72×5.34 mm and 10.17×8.69×7.09 mm; the shape distribution of rice and wheat is spindle-shaped with length × width × thickness of 7.07×3.48×2.37 mm and 6.01×3.43×3.25 mm, respectively, the shape of soybeans is nearly spherical, with a length × width × thickness of 7.04×6.65×6.22 mm.

Discrete element method

EDEM2020 of Altair Engineering, Inc., was used to numerically simulate the AoR of fertiliser particles. Since the moisture content of selected seeds is low, the Hertz-Mindlin (no-slip) contact model was adopted to calculate the contact between particle-particle and particle-geometry interactions shown in Figure 4. Hertz-Mindlin (no-slip) is the default model used in EDEM, accurate and efficient in force calculation. This model's normal force component is based on Hertzian contact theory (Hertz, 1881). The tangential force model is based on the research work of Mindlin-Deresiewicz (Mindlin, 1949; Mindlin and Deresiewicz, 1953). As described in the literature (Tsuji *et al.*, 1992), both normal and tangential forces have damping components, and the damping coefficient is related to the restitution coefficient. Tangential friction complies with Coulomb's law of friction reference (Cundall and Strack, 1979). The contact-independent directional constant torque model realises the rolling friction force, referring to the literature (Sakaguchi *et al.*, 1993).

In particular, the normal force Fn is a function of the normal overlap amount δn, and the expression is as follows,

$$F_n = \frac{4}{3} E^* \sqrt{R^*} \delta_n^{\frac{3}{2}} \tag{1}$$

Among them, when Young's modulus E^*, equivalent radius R^* is defined as:

$$\frac{1}{E^*} = \frac{1-v_i^2}{E_i} + \frac{1-v_j^2}{E_j} \tag{2}$$

$$\frac{1}{R^*} = \frac{1}{R_i} + \frac{1}{R_j} \tag{3}$$

E_i, v_i, R_i, and E_j, v_j, R_j are Young's modulus, Poisson's ratio, and the radius of the contact sphere, respectively.

In addition, the expression of the damping force F_n^d is:

$$F_n^d = -2\sqrt{\frac{5}{6}}\beta\sqrt{S_n m^*}\, v_n^{\overline{rel}} \tag{4}$$

Among them $v_n^{\overline{rel}}$ is the normal component of the relative velocity, m^*, β, and S_n are the equivalent mass, damping coefficient, and normal stiffness, respectively, defined as:

$$m^* = \frac{m_i m_j}{m_i + m_j} \tag{5}$$

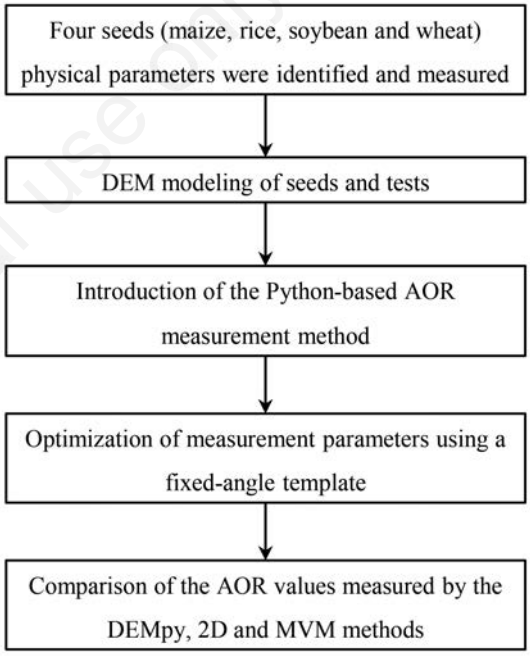

Figure 2. Flow chart of research ideas. DEM, discrete element methods; AoR, angle of repose; MVM, manual measurements using a virtual protractor.

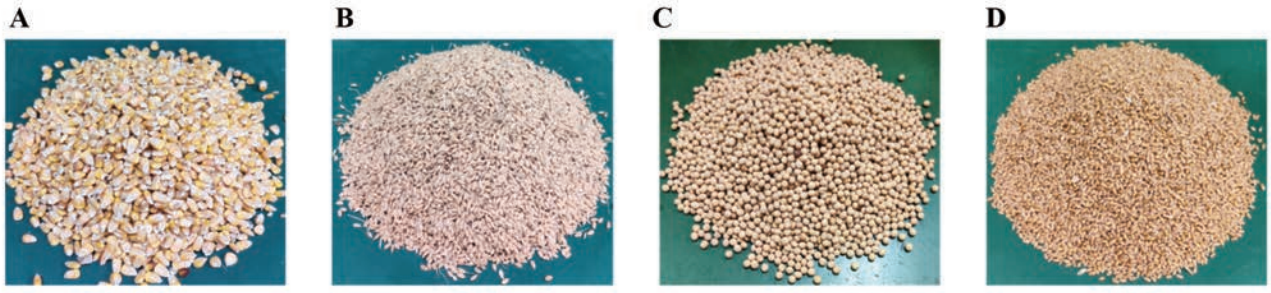

Figure 3. Photos of seeds used in the case study: **A**) maize; **B**) rice; **C**) soybeans; **D**) wheat.

$$\beta = \frac{\ln e}{\sqrt{\ln^2 e + \pi^2}} \quad (6)$$

$$S_n = 2E^* \sqrt{R^* \delta_n} \quad (7)$$

e is the coefficient of restitution. The tangential force F_t depends on the tangential overlap amount δ_t and the tangential stiffness S_t.

Among them:

$$S_t = 8G^* \sqrt{R^* \delta_n} \quad (8)$$

G^* is the equivalent shear modulus. In addition, the expression of tangential damping is:

$$F_t^d = -2\sqrt{\frac{5}{6}}\beta\sqrt{S_t m^*}\, v_t^{rel} \quad (9)$$

is the tangential component of the relative velocity. The tangential force is limited by the Coulomb friction $\mu_s F_n$, where μ_s is the static friction coefficient.

For simulation, rolling friction is essential and is considered by applying a moment on the contact surface.

$$\tau_i = -\mu_r F_n R_i \omega_i \quad (10)$$

Among them, μ_r is the coefficient of rolling friction, R_i is the distance from the contact point to the centre of mass, and ω_i is the unit angular velocity vector at the contact point.

Simulation setup in EDEM2020

In DEM simulation, the shape of seed particles is combined from multiple spheres, allowing for significant overlap (as shown in Figures 4D and 5A). Maize grain, with 70% flat seeds and 30% round seeds, is filled with 10 and 8 spheres, respectively. Rice, soybean, and wheat are supplied with 7, 2, and 7 spheres, respectively. The piled cone forming method applied here is to lift a bottomless cylinder (Figure 5E), whose basic form was previously introduced by Wu *et al*. (2011). The simulation of the AoR test started with the generation of an assembly of particles within a virtual particle factory. In this case, the factory was located at the top of the cylinder, and the resulting particles fell by gravity. The diameter and height of the cylinder are 90 mm and 300 mm, respectively. The number of maize, rice, soybean, and wheat grains contained in the cylinders were 5172, 22970, 7785, and 28588, respectively. In addition, the diameter of the plate that receives the particles to form the pile is 250 mm. After the cylinder is filled with particles, the cylinder is lifted upward at a speed of 30 mm/s. Then, the particles start to flow, forming a self-organising cone. The simulation was completed when the particles settled again.

The calculation capability was assessed using a workstation (DELL Precision T7920). The total simulation time is 5 s, and the time step is 5×10^{-6} s. Save data every 0.01 s. The particle-particle and wall-particle contact parameters [including coefficient of restitution (CoR), coefficient of static friction (CoSF), and coefficient of rolling friction (CoRF)] used in the simulation are shown in Table 2.

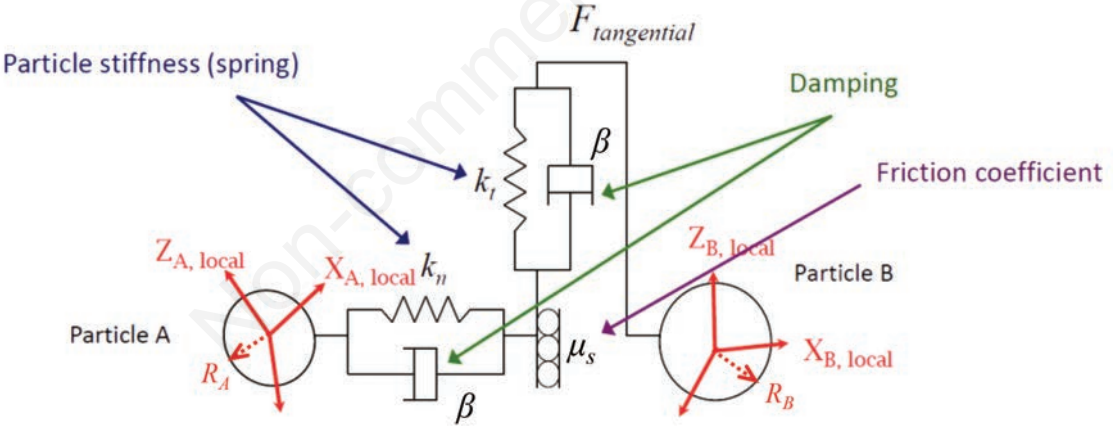

Figure 4. Hertz-Mindlin (no-slip) contact model in EDEM2020.

Table 2. Fixed contact parameters of simulated particles with wall and particles.

Parameters	Soybean (Jia *et al.*, 2018)	Rice (Lu *et al.*, 2016)	Wheat (Liu *et al.*, 2019)	Maize (Ding *et al.*, 2019)
CoR - PW	0.6	0.52	0.42	0.182
CoSF - PW	0.3	0.5	0.53	0.431
CoRF - PW	0.1	0.1	0.07	0.078
CoR - PP	0.6	0.3	0.51	0.621
CoSF - PP	0.5	0.56	0.55	0.459
CoRF - PP	0.01	0.15	0.05	0.093

The methodology for the determination of angle of repose

After completing the simulation, run the AoR post-processing program based on Python 3.6 to connect the EDEMpy library. The whole data processing process consists of three steps, as shown in Figure 6.

Firstly, the particles of the simulated bulk pile are extracted. Since the data storage format in EDEM2020 is H5, the particle coordinate information can be read by calling the h5py package in Python 3.6. The coordinates of the centre of the particle population on plate O are then obtained, as shown in Figure 6A.

Secondly, the particle pile is evenly divided into n parts every θ degree (Figure 6B), and n particle slices are obtained, then find the coordinates of the outermost particles of the particles population for a particular slice (Figure 6C), then divide each slice into two parts, low domain D_2-D_1 and high domain D_1, divide low domain D_2-D_1 into m bins every D_3, and obtain the coordinates of the outermost particles within each bin separately (Figure 6D). A linear fit to the particle coordinates in m bins (Figure 6E) is performed as follows. Suppose the coordinates of the m particles are (x_i, z_i), i=0, 1, … , m-1. To fit the straight line $p(x) = a + bx$, the mean square error is:

$$Q(a,b)=\sum_{i=0}^{m-1}\left(p(x_i)-z_i\right)^2=\sum_{i=0}^{m-1}\left(a+bx_i-z_i\right)^2 \tag{11}$$

In calculus theory, the minimal value of $Q(a, b)$ has to satisfy:

$$\begin{cases}\dfrac{\partial Q(a,b)}{\partial a}=2\sum_{i=0}^{m-1}\left(a+bx_i-z_i\right)\\ \dfrac{\partial Q(a,b)}{\partial b}=2\sum_{i=0}^{m-1}\left(a+bx_i-z_i\right)x_i=0\end{cases} \tag{12}$$

The normal equation of the fitted curve is obtained after rectification:

$$\begin{cases}ma+b\sum_{i=0}^{m-1}x_i=\sum_{i=0}^{m-1}z_i\\ a\sum_{i=0}^{m-1}x_i+b\sum_{i=0}^{m-1}x_i^2=\sum_{i=0}^{m-1}x_iz_i\end{cases} \tag{13}$$

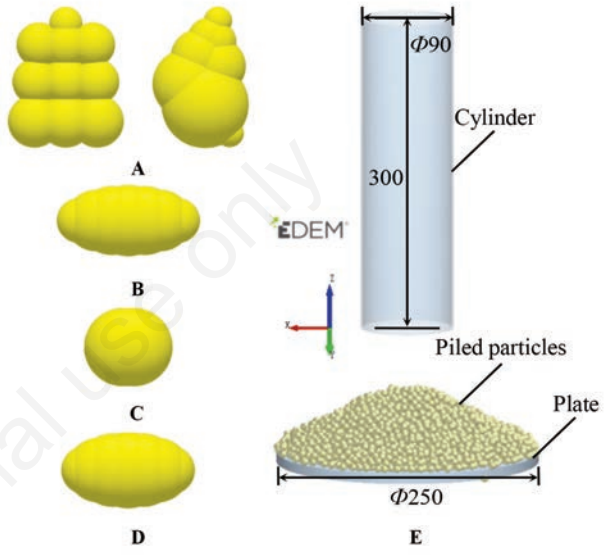

Figure 5. Photos of seeds used in EDEM2020: **A**) maize; **B**) rice; **C**) soybeans; **D**) wheat; **E**) simulation set-up.

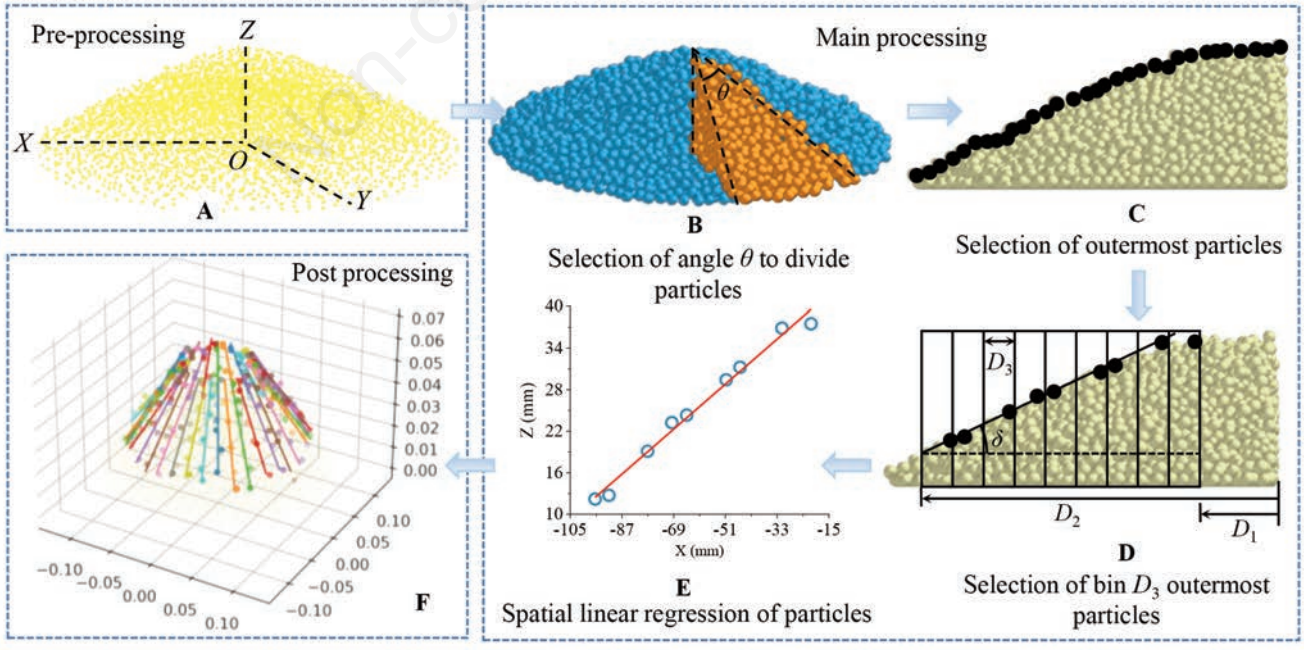

Figure 6. Flowchart of the data processing method.

Solve the equation by the elimination method or Klemm's method:

$$a = \left(\sum_{i=0}^{m-1} z_i \sum_{i=0}^{m-1} x_i^2 - \sum_{i=0}^{m-1} x_i \sum_{i=0}^{m-1} x_i z_i\right) \Big/ \left(m \sum_{i=0}^{m-1} x_i^2 - \left(\sum_{i=0}^{m-1} x_i\right)^2\right)$$
$$b = \left(m \sum_{i=0}^{m-1} x_i z_i - \sum_{i=0}^{m-1} x_i \sum_{i=0}^{m-1} z_i\right) \Big/ \left(m \sum_{i=0}^{m-1} x_i^2 - \left(\sum_{i=0}^{m-1} x_i\right)^2\right) \quad (14)$$

The degree δ of AoR is calculated as:

$$\delta = \arctan b \frac{180^\circ}{\pi} \quad (15)$$

Lastly, the AoR of multiple slices is counted to obtain the mean value and standard deviation, then draw 3D graphics of fitted lines and particles, as shown in Figure 6F.

Experimental validation

The developed method was validated and evaluated in two steps. In the first step, the developed algorithm was calibrated with four 36° angled 3D cone shape templates populated with maize, rice, soybeans, and wheat (Figure 7A-D). Then, the effects of the number of particle slices (n) and sampling bin diameter (D_3) on the accuracy of angle measurements were examined comprehensively. As a result, the curves are obtained as described in 2.4, as shown in Figure 7E. Then we can get the optimum value of the number of particle slices (n) and sampling bin diameter (D_3) when we use the novel method to measure the AoR of granular seeds in EDEM.

In the second step, the AoR tests of maize, rice, soybean, and wheat were conducted under different CoSFs and CoRFs. First, the mean and standard deviation of AoR of maize, rice, soybean, and wheat were obtained using the algorithm described in this paper (DEMpy), digital image analysis (2D), and manual measurements using a virtual protractor (MVM), respectively. Then the linear models and correlation coefficients were fitted between CoSFs and CoRFs and the mean AoR values of different seeds. Finally, the AoR values under different CoSFs and CoRFs were predicted based on the linear models and compared with the actual AoR values obtained from simulations to verify the reliability and accuracy of the algorithm described in this paper.

Results and Discussion

Calibration of D_3 and n on the accuracy of angles measurement

Nine different values of n and D_3 are selected to discuss whether the results from the algorithm described in this paper depend on the number of particle slices (n) and the sampling bin diameter (D_3). The results are presented in Figures 8 and 9.

As shown in Figure 8, the D_3 values of maize, rice, soybean, and wheat were set to 12 mm, 9 mm, 8 mm, and 9 mm. When the value of n gradually increased from 4 to 36, the values of the angle obtained by the algorithm tended to 36° for soybean and wheat. In contrast, for maize, when the value of n gradually increases from 4 to 32, the angle value gradually increases, tending to 36°, and then gradually decreases when the value of n continues to increase. For rice, when the value of n gradually increases from 4 to 28, the angle value gradually decreases, tending to 36°, and then increases when the value of n continues to increase. When the relative error between the angle measured by the program and the actual angle of the 3D template was minimal, the n values were 32, 28, 36, and 36 for corn, rice, soybean, and wheat, respectively.

As shown in Figure 9, the n values of maize, rice, soybean, and wheat were set to 32, 28, 36, and 36. As the D_3 value increases from 6 to 14, the maize angle measured by the program gradually increases and tends to 36°. As the D_3 value increased from 4 to 12, the relative errors between the program-measured rice, soybean, wheat, and the 3D template angles decreased and then increased. When the relative errors were the smallest for maize, rice, soybean, and wheat, the corresponding D_3 values were 14, 9, 10, and 9.

In summary, the relative error between the values of the angle obtained by the algorithm and the theoretical values was the smallest when the n values of maize, rice, soybean, and wheat were 32, 28, 36, and 36, and the D_3 values were 14 mm, 9 mm, 10 mm, and 9 mm, the algorithm was most accurate to calculate the particles angles in EDEM.

Impact of angle of repose measurement accuracy compared to other methods

In this section, three methods: the algorithm presented in this paper (DEMpy), digital image analysis (2D), and MVM, will be used to measure the AoR obtained from the simulation experiments, respectively. The values of n and D_3 when measuring the

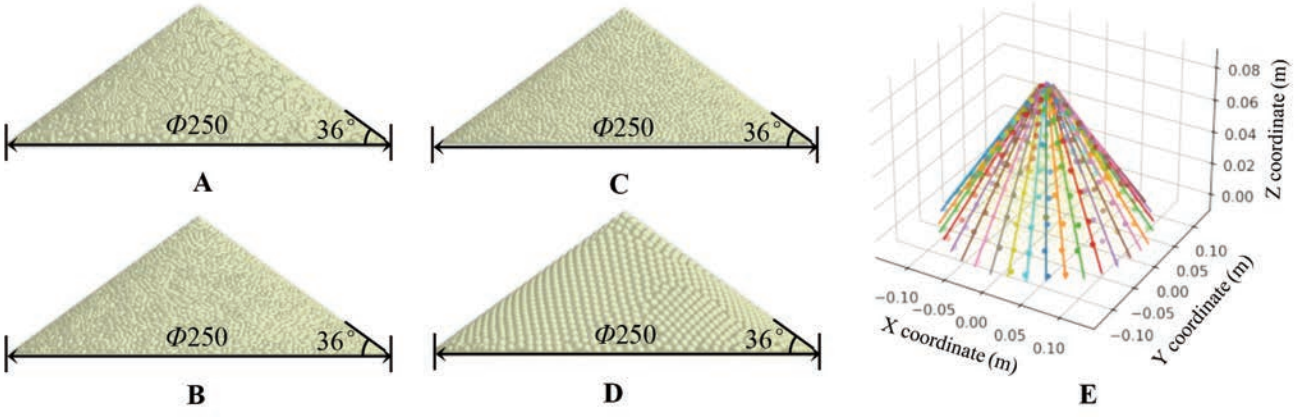

Figure 7. 3D template for input parameters optimisation in the EDEM2020: **A**) maize; **B**) rice; **C**) soybeans; **D**) wheat; **E**) fitted line graph.

simulated AoR of maize, rice, soybean, and wheat using DEMpy are referenced to 3.1. The sample size for estimating the AoR of a single heap using MVM and 2D is 10 and 5 in this paper. Because Frączek *et al*. (2007) reported that minimum sample sizes of 3-10 and 2-5 for AoR can be accurately obtained using MVM and 2D.

Mean and standard deviation of angle of repose

The relationship between the CoSF and the AoR between different seeds is shown in Figure 10. The values of CoR and CoRF are shown in Table 2. The CoSF of AoR for maize, rice, soybean, and wheat ranged from 0.376 to 0.536, 0.2 to 0.6, 0.4 to 0.8, and 0.3 to 0.7, respectively. After three repeats of the simulation were completed, the AoR was calculated using three methods: DEMpy, 2D, and MVM. As can be seen from Figure 10, the AoR gradually increases with the increase of CoSF. In most cases, the AoR obtained for 2D is slightly higher than that of MVM. The standard deviation obtained for 2D is marginally smaller than the standard deviation of MVM. This result is consistent with the results obtained from Fraczek *et al*.'s study (2007). In addition, there is no significant difference between the AoR and standard deviation obtained from 2D and DEMpy. For CoRF, a similar phenomenon can be derived in Figure 11, the AoR values measured by all three methods increased with increasing CoRF, but the AoR values measured by 2D and DEMpy were not significantly different. However, they were significantly larger than those measured by MVM, and comparing the standard deviation, it can be seen that the standard

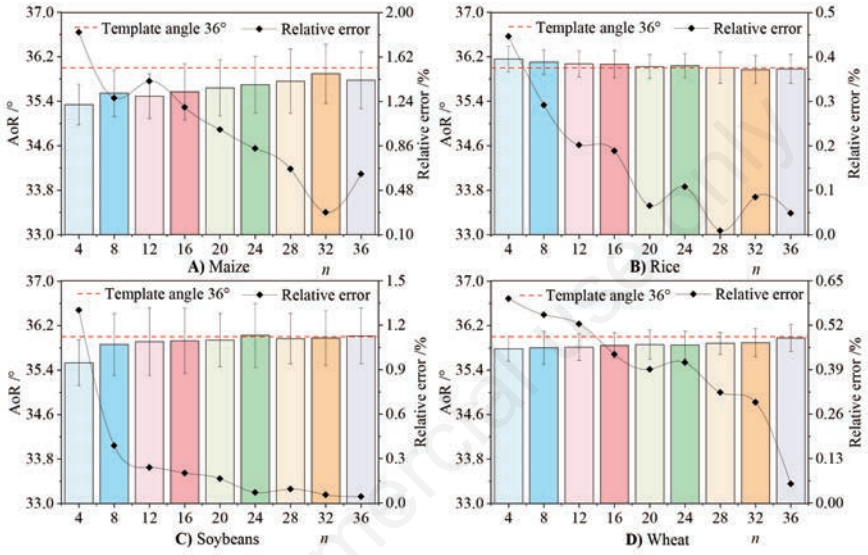

Figure 8. Means and standard deviations of angles of repose (AoR), relative error between measured and actual values for varied sample amounts (*n*).

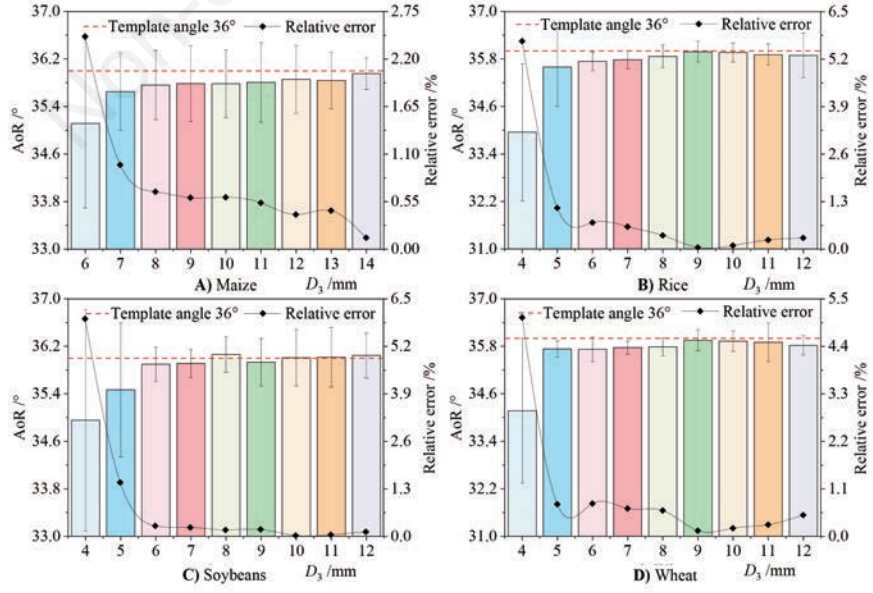

Figure 9. Means and standard deviations of angles of repose (AoR), relative error between measured and actual values for varied sample bin diameter (D_3).

deviation of the AoR values measured by MVM is larger, indicating that the data obtained by MVM is less stable compared with 2D and DEMpy. It shows that the same accuracy as a 2D measurement of AoR can be obtained when using DEMpy to measure AoR in DEM.

The linear model of angle of repose with coefficient of static and rolling friction

A least-squares regression was performed on the CoSF, and CoRF obtained with the AoR data to determine whether AoR has a linear relationship with CoSF and CoRF, and the results are shown in Figures 12 and 13. As can be seen from Figures 12 and 13, AoR was observed to vary essentially linearly with CoSF and CoRF, consistent with the findings of Han *et al*. (2014). The correlation coefficients R^2 of AoR with CoSF and CoRF obtained from the three measurement methods of DEMpy, 2D, and MVM are all greater than 0.95, indicating the linear fit of AoR with CoSF and CoRF is high. Furthermore, the R^2 obtained by DEMpy and 2D is more significant than the R^2 obtained by MVM. This is because the AoR obtained by MVM mixed with human subjective judgment increases the uncertainty of the measurement results. On the other

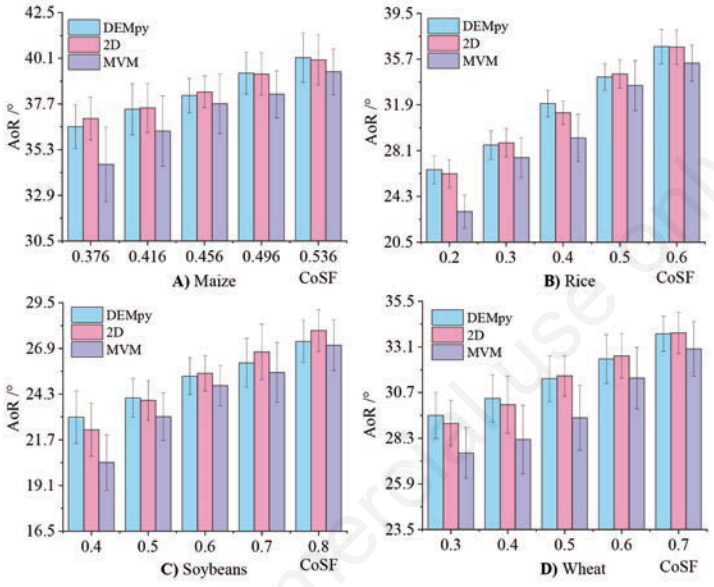

Figure 10. Relationship between coefficient of static friction (CoSF) and angle of repose (AoR) for different seeds: **A**) maize; **B**) rice; **C**) soybean; and **D**) wheat. DEM, discrete element methods; MVM, manual measurements using a virtual protractor.

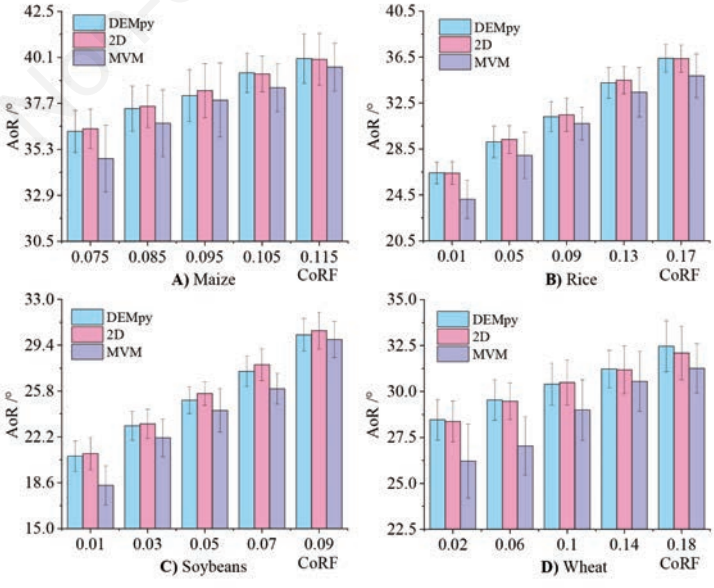

Figure 11. Relationship between coefficient of rolling friction (CoRF) and angle of repose (AoR) for different seeds: **A**) maize; **B**) rice; **C**) soybean; **D**) wheat. DEM, discrete element methods; MVM, manual measurements using a virtual protractor.

hand, measuring AoR with DEMpy and 2D is almost fully automatic, which avoids personal human judgment and improves the consistency and accuracy of measurement. Therefore, the AoR obtained by DEMpy and 2D is closer to the valid AoR, and the correlation coefficient R^2 is tendency 1. In general, both DEMpy and 2D methods are basically the same in terms of AoR measurement accuracy; both are significantly more stable and have less error than the AoR values measured by MVM.

The relative error between predicted and simulated angle of repose

To further confirm the authenticity and reliability of the AoR obtained by DEMpy, 2D, and MVM, the prediction of AoR was performed according to the linear fitting equations obtained by each method, respectively. First, the prediction point was selected as the average value between each adjacent two CoSFs in Figure 12 and CoRFs in Figure 13. Then, the relevant parameters were

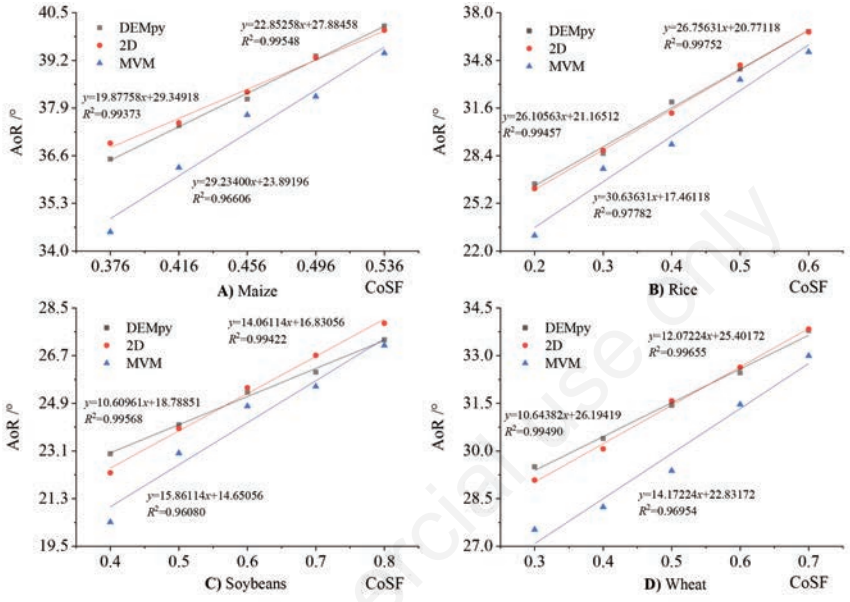

Figure 12 Fitted lines between coefficient of static friction (CoSF) and angle of repose (AoR) for different seeds: **A**) maize; **B**) rice; C) soybean; **D**) wheat. DEM, discrete element methods; MVM, manual measurements using a virtual protractor.

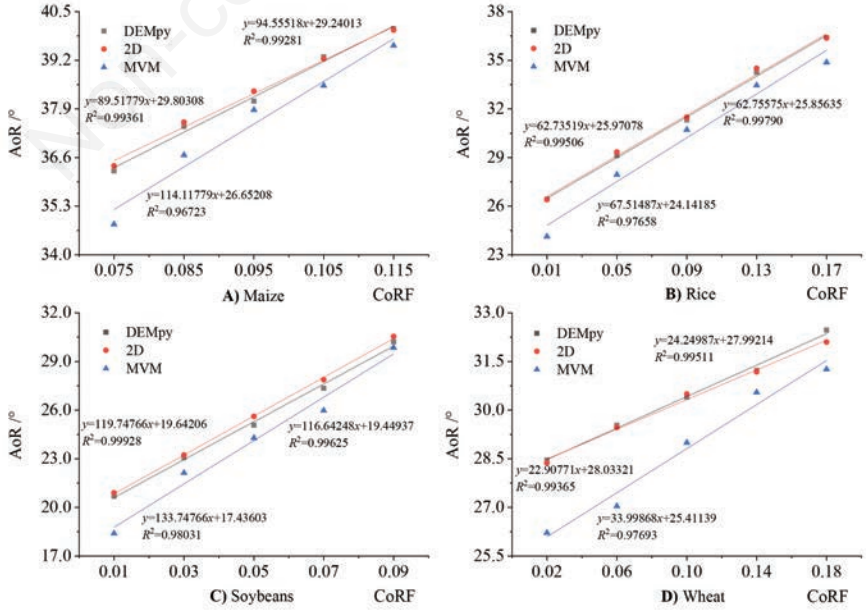

Figure 13. Fitted lines between coefficient of static friction (CoSF) and angle of repose (AoR) for different seeds: **A**) maize; **B**) rice; **C**) soybean; **D**) wheat. DEM, discrete element methods; MVM, manual measurements using a virtual protractor.

substituted into EDEM for simulation tests. Finally, the AoR was measured by DEMpy, 2D, and MVM methods, respectively, to compare the relative errors of the predicted AoR and the simulated AoR, as shown in Figures 14 and 15.

As shown in Figures 14 and 15, for the relative error between the predicted AoR and the simulated AoR, DEMpy, and 2D are smaller than MVM. On the one hand, the correlation coefficients of the fitted equations obtained by DEMpy and 2D are significant, so the predicted values are closer to the simulated values; On the other hand, the AoR values obtained by MVM have an extensive range and uncertainty, which increases the chance of error.

For DEMpy and 2D, the consistency and accuracy of the obtained AoR are high because both methods avoid the interference of human subjective factors. Since 2D has to open and read the data file in EDEM first, this process takes about 10s, then artificially get 5 pictures of particle piles, this process takes about 30 s ~50 s, then use MATLAB or other software to analyse the pictures, which takes 1 s ~2 s, while DEMpy uses Python to read the

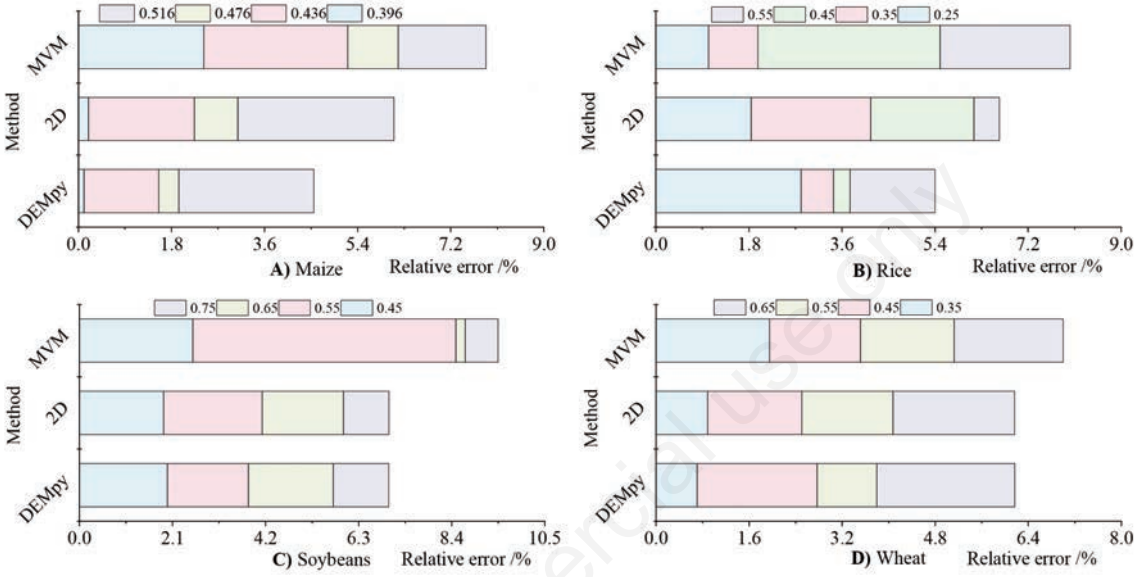

Figure 14. Relative error between predicted and simulated angle of repose for different seeds: **A**) maize; **B**) rice; **C**) soybean; **D**) wheat at different coefficient of static friction. DEM, discrete element methods; MVM, manual measurements using a virtual protractor.

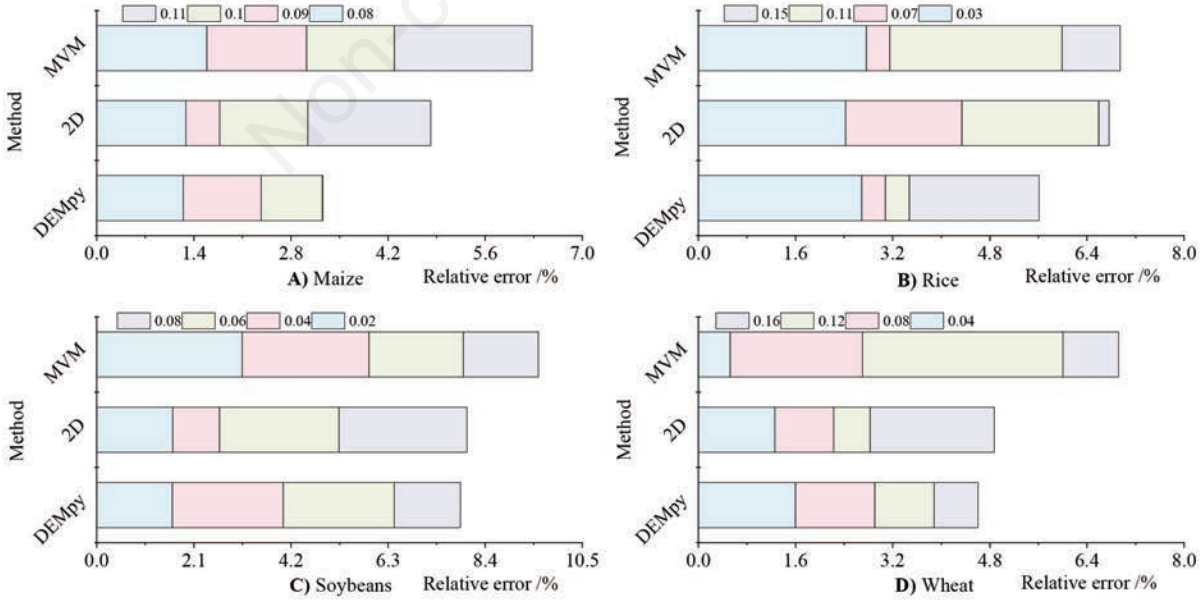

Figure 15. The relative error between predicted and simulated angle of repose for different seeds: **A**) maize; **B**) rice; **C**) soybean; **D**) wheat at different coefficient of rolling friction. DEM, discrete element methods; MVM, manual measurements using a virtual protractor.

particle coordinate information directly and convert and fit the coordinate information, the total time is less than 2 s, so using DEMpy to measure AoR can significantly reduce the time consumption and improve the efficiency of scientific research.

Conclusions

This study presents a fully automated and consistent method to measure the AoR of granular materials in DEM software using linear regression analysis and particle coordinate acquisition algorithm based on Python.

The AoR values measured by DEMpy, 2D, and MVM were compared, and it was found that the mean and standard deviation of the measured AoR, the fit to CoRF and CoSF, and the relative errors of the predicted and simulated values were basically the same for DEMpy and 2D, and all had better consistency and stability compared with the AoR values measured by MVM.

From an operational point of view, the time consumption for obtaining AoR using DEMpy measurements is much less than that of 2D so that DEMpy can be used instead of 2D for automatic measurement of AoR in DEM software post-processing.

References

Cao X., Li Z., Li H., Wang X., Ma X. 2021. Measurement and calibration of the parameters for discrete element method modeling of rapeseed. Processes 9:605.

Cheng N., Zhao K. 2017. Difference between static and dynamic angle of repose of uniform sediment grains. Int. J. Sediment Res. 32:149-54.

Cundall P.A., Strack O.D.L. 1979. A discrete numerical model for granular assemblies. Géotechnique 29:47-65.

Ding L., Yang L., Zhang D., Cui T., Gao X. 2019. Design and experiment of seed plate of maize air suction seed metering device based on DEM-CFD. Trans. Chinese Soc. Agric. Machine. 50:50-60.

Frączek J., Złobecki A., Zemanek J. 2007. Assessment of angle of repose of granular plant material using computer image analysis. J. Food Engine. 83:17-22.

Gao X., Cui T., Zhou Z., Yu Y., Xu Y., Zhang D. 2021. DEM study of particle motion in novel high-speed seed metering device. Adv. Powder Technol. 32:1438-49.

Geldart D., Abdullah E.C., Hassanpour A., Nwoke L.C., Wouters I. 2006. Characterization of powder flowability using measurement of angle of repose. China Partic. 4:104-7.

Han Y., Jia F., Tang Y., Liu Y., Zhang Q. 2014. Influence of granular coefficient of rolling friction on accumulation characteristics. Acta Phys. Sinica 63:173-9.

Hertz H. 1881. On the contact of elastic solids. J. Reine Angew. Math. 92:156-71.

Hu H., Zhou Z., Wu W., Yang W., Li T., Chang C. 2021. Distribution characteristics and parameter optimisation of an air-assisted centralised seed-metering device for rapeseed using a CFD-DEM coupled simulation. Biosyst. Engine. 208:246-59.

Jia H., Chen Y., Zhao J., Wang X., Guo M., Zhuang J. 2018. Design and experiment of pneumatic-mechanical combined precision metering device for soybean. Trans. Chinese Soc. Agric. Machin. 49:75-86.

Kalman H., Portnikov D. 2021. Analyzing bulk density and void fraction: B. Effect of moisture content and compression pressure. Powder Technol. 381:285-97.

Klanfar M., Korman T., Domitrović D., Herceg V. 2021. Testing the novel method for angle of repose measurement based on area-weighted average slope of a triangular mesh. Powder Technol. 387:396-405.

Li C., Honeyands T., O'Dea D., Moreno-Atanasio R. 2017. The angle of repose and size segregation of iron ore granules: DEM analysis and experimental investigation. Powder Technol. 320:257-72.

Li P., Ucgul M., Lee S., Saunders C. 2020. A new approach for the automatic measurement of the angle of repose of granular materials with maximal least square using digital image processing. Comput. Electron. Agric. 172:105356.

Liu C., Wei D., Du X., Jiang M., Song J., Zhang F. 2019. Design and test of wide seedling strip wheat precision hook-hole type seed-metering device. Trans. Chinese Soc. Agric. Machine. 50:75-84.

Liu C., Wei D., Song J., Li Y., Du X., Zhang F. 2018. Systematic study on boundary parameters of discrete element simulation of granular fertilizer. Trans. Chinese Soc. Agric. Machine. 50:82-9.

Lu F., Ma X., Qi L., Tan S., Tan Y., Jiang L., Sun G. 2016. Parameter optimization and experiment of vibration seed-uniforming device for hybrid rice based on discrete element method. Trans. Chinese Soc. Agric. Engine. 32:17-25.

Marigo M., Stitt E.H. 2015. Discrete element method (DEM) for industrial applications: comments on calibration and validation for the modelling of cylindrical pellets. Kona 32:236-52.

Mindlin R.D. 1949. Compliance of elastic bodies in contact. J. Appl. Mechan.-Transa. ASME 16:259-68.

Mindlin R.D., Deresiewicz H. 1953. Elastic spheres in contact under varying oblique forces. ASME September:327-44.

Mousaviraad M., Tekeste M.Z. 2020. Effect of grain moisture content on physical, mechanical, and bulk dynamic behaviour of maize. Biosyst. Engine. 195:186-97.

Qi L., Chen Y., Sadek M. 2019. Simulations of soil flow properties using the discrete element method (DEM). Comput. Electron. Agric. 157:254-60.

Rackl M., Grötsch F.E., Rusch M., Fottner J. 2017. Qualitative and quantitative assessment of 3D-scanned bulk solid heap data. Powder Technol. 321:105-18.

Roessler T., Katterfeld A. 2018. Scaling of the angle of repose test and its influence on the calibration of DEM parameters using upscaled particles. Powder Technol. 330:58-66.

Sakaguchi H., Ozaki E., Igarashi T. 1993. Plugging of the flow of granular materials during the discharge from a silo. Int. J. Modern Phys. B 7:1949.

Sun K., Yu J., Liang L., Wang Y., Yan D., Zhou L. 2022. A DEM-based general modelling method and experimental verification for wheat seeds. Powder Technol. 401:117353.

Tan Y., Fottner J., Kessler S. 2020. An efficient and reliable method for determining the angle of repose of biomass by using 3D scan. Biomass Bioener. 132:105434.

Wang Y., Li H., Hu H., He J., Wang Q., Lu C. 2022. A noncontact self-suction wheat shooting device for sustainable agriculture: a preliminary research. Comput. Electron. Agricult. 197:106927.

Wang Y., Zhang D., Yang L., Cui T., Jing H., Zhong X. 2020. Modeling the interaction of soil and a vibrating subsoiler using the discrete element method. Comput. Electron. Agric. 174:105518.

Wójcik A., Klapa P., Mitka B., Piech I. 2019. The use of TLS and

UAV methods for measurement of the repose angle of granular materials in terrain conditions. Measurement 146:780-91.
Wu M.R., Schott D.L., Lodewijks G. 2011. Physical properties of solid biomass. Biomass Bioener. 35:2093-105.
Zhu Q., Wu G., Chen L., Zhao C., Meng Z. 2018. Influences of structure parameters of straight flute wheel on fertilizing performance of fertilizer apparatus. Trans. Chinese Soc. Agric. Engine. 34:12-20.